biologia plantarum
an international journal for experimental botany

BIOLOGIA PLANTARUM (2026) 70: 11-17 DOI: 10.32615/bp.2026.002

RT-qPCR analysis of genotype-specific beet yellows virus accumulation in sugar beet

Emad IBRAHIM[1], Dilara BOZDOĞAN[1,2], and Jiban KUMAR KUNDU[1,*]

[1] *Plant Virus and Vector Interactions, Czech Agrifood Research Center (CARC), Drnovská 507, 16106 Prague, Czech Republic*
[2] *Department of Plant Protection, Faculty of Agrobiology, Food and Natural Resources, Czech University of Life Sciences Prague, Kamýcká 129, 16500 Prague, Czech Republic*

[*]Corresponding author: E-mail: jiban.kumar@carc.cz

Abstract

Background: Rapid and objective characterisation of viral accumulation requires methods combining fast detection and temporal resolution.
Aims: Develop a two-phase approach for screening sugar beet genotypes for beet yellows virus (BYV) accumulation dynamics.
Methods: Phase 1 employed one-enzyme RTX-PCR for rapid BYV detection, followed by single-time-point RT-qPCR at 30 days post-inoculation (dpi) to screen ten genotypes. Phase 2 performed time-course RT-qPCR at six time points (10-60 dpi) on two contrasting genotypes selected from Phase 1, with assay performance validated by a standard curve.
Results: One-enzyme RTX-PCR confirmed BYV infection, enabling quantification; single-time-point RT-qPCR at 30 dpi showed a 5.7-fold titre range (5.6×10^7 to 3.2×10^8 copies), while time-course RT-qPCR revealed distinct trajectories, relatively resistant GZs1 increased gradually (~5.0×10^5 at 10 dpi to 1.7 - 2.3 $\times 10^7$ at 40 - 60 dpi) whereas susceptible Masaryk rose rapidly early (~3.1×10^6 at 10 dpi) and peaked at 3.7×10^7 by 40 dpi, dynamics not captured by single-time-point measurements; standard curve metrics indicated high assay quality (R^2 = 0.9976; efficiency = 103%).
Conclusions: This two-phase method combines speed with precision for effective genotype comparison. It reveals BYV accumulation dynamics that are not captured by single-point assays.

Keywords: Beet yellows virus, kinetics, RT-qPCR, RTX-PCR, sugar beet, viral quantification.

Introduction

Sugar beet (*Beta vulgaris* L.) is a globally important crop cultivated primarily for sugar production. Sugar beet plays a critical role in the sugar industry in temperate regions (Sun et al., 2024). This economic significance underscores the need to address threats to crop productivity, particularly virus yellows (VY). The most destructive pathogens associated with VY in recent European outbreaks are aphid-transmitted viruses, chiefly the beet yellows virus (BYV; genus *Closterovirus*) (Hossain et al., 2021). BYV is a positive-strand RNA virus transmitted by the green peach aphid (*Myzus persicae*), which facilitates rapid field-to-field spread under favourable environmental conditions

Received 22 December 2025, *last revision* 2 February 2026, *accepted* 4 February 2026.
Abbreviations: AAFP - acquisition access feeding period; BYV - beet yellows virus; dpi - days post-inoculation; IAFP - inoculation access feeding period; one-enzyme RTX-PCR - PCR using RTX enzyme for one enzyme RT-PCR; RT-qPCR - reverse transcription, quantitative polymerase chain reaction.
Acknowledgements: We thank Markéta Vítámvásová and Hana Novotná (Plant Virus and Vector Interactions, Czech Agrifood Research Center, Czech Republic) for their excellent technical assistance. We also thank Dr. Britt-Lousie Lennefors (United Beet Seeds, Tienen, Belgium) for providing two sugar beet genotypes. This work was supported by project no. FW04020104 from Technology Agency of the Czech Republic.
Data and materials availability statement: Data and materials will be available under reasonable request to the corresponding author.
Conflict of interest: The authors declare that they have no conflict of interest.

(Jiménez et al., 2018; Hossain et al., 2024). BYV causes characteristic leaf yellowing with reddish-brown necrotic spots on older leaves, reduced photosynthesis, and decreased green leaf area, resulting in substantial yield loss (Hossain et al., 2024). Yield losses due to BYV infections have been quantified at 24 - 47%, depending on the timing of infection during the growing season, with white sugar yield reductions being especially severe when infection occurs early (Smith and Hallsworth, 1990; Borgolte et al., 2024).

Insecticides targeting the aphid vector *M. persicae* are ineffective because small populations still transmit BYV efficiently (Bass et al., 2014). The 2018 EU neonicotinoid ban intensified outbreaks (Hossain et al., 2021). Host–plant resistance is now the preferred approach. It reduces pesticide use, limits virus spread, and improves resilience, although BYV resistance sources remain limited (Kumar et al., 2022; 2023). To develop and understand resistance, reliable virus detection and quantification methods are needed, in addition to visual scoring.

Accurate and rapid quantification of plant viruses is essential for diagnostics, germplasm evaluation, and host–pathogen interaction studies (Kanapiya et al., 2024). As no single assay captures all relevant information, complementary detection methods are required. One-step RTX-PCR and RT-qPCR have advanced the detection of plant viruses (Kumar et al., 2023; Kanapiya et al., 2024). One-step RTX-PCR uses a single enzyme for reverse transcription and DNA amplification. This reduces assay time and cost while maintaining sensitivity comparable to that of ELISA and conventional RT-PCR (Hoffmeisterová et al., 2022). The binary output confirmed the presence or absence of viral genomes and served as a quality control step before quantitative analysis. RT-qPCR provides precise measurements of viral genome copy numbers. A single-time-point assay enables rapid comparison of genotypes based on viral load and supports early-stage screening (Alquicer et al., 2023; Ibrahim et al., 2023; Sharaf et al., 2023). However, such measurements capture only a static state and cannot resolve the infection dynamics. Time-course RT-qPCR provides this missing dimension to the study. Repeated measurements reveal the timing of infection, the strength and speed of host responses, and the trajectory of disease progression (Lough et al., 2015; Vegvari et al., 2016). These kinetic profiles distinguish biological processes that remain hidden from single snapshots (Withycombe et al., 2024).

In this study, we applied a two-phase framework to quantify BYV accumulation in sugar beet, combining rapid RTX-PCR confirmation with RT-qPCR. Single-time-point screening after 30 days post-inoculation (dpi) across 10 genotypes and a six-point time course (10 - 60 dpi) in two contrasting genotypes resolved genotype-dependent accumulation kinetics.

Materials and methods

Plant material and virus sources: The present study was conducted to evaluate the resistance of ten *B. vulgaris* genotypes to BYV under both controlled greenhouse and field conditions. The sugar beet genotypes were evaluated under greenhouse conditions and include: Briga (KWS), Eliška (KWS), GZs1 (United Beet Seeds, Tienen, Belgium), GZs2 (United Beet Seeds, Tienen, Belgium), Laser (DLF Beet Seed ApS), Masaryk (Strube CZ), Regalis (DLF Beet Seed ApS), Silvana (KWS), Viola (KWS), and 4K576 (KWS). The BYV isolate used in this study was a field isolate maintained in the laboratory at the Czech Agrifood Research Center (CARC). The virus isolate was continuously maintained on sugar beet plants under greenhouse conditions at 20 - 22°C day/16°C night, a 16-h photoperiod, and 70% relative humidity. All tested genotypes were artificially inoculated with the BYV isolate using viruliferous aphids, *M. persicae*.

Plant growth and virus inoculation: Seeds of the sugar beet cultivars were sown in soil-filled pots and maintained in an insect-proof greenhouse under controlled environmental conditions mentioned above. Virus-free aphids (*M. persicae*) were reared on Chinese cabbage (*Brassica rapa*) in insect-proof cages. Before inoculation, aphids were placed on BYV-infected sugar beet plants for three days of the acquisition access feeding period (AAFP). When seedlings reached the four-leaf stage, viruliferous aphids were transferred to experimental plants (approximately five aphids per plant) for a three-day inoculation access feeding period (IAFP). Aphid feeding activity was subsequently inactivated with insecticide (acetamiprid 0.25 mL/L H_2O). Untreated control plants were maintained in aphid-free greenhouse conditions. All plants were maintained in separate insect-proof net cages under greenhouse conditions to allow symptom expression. Leaf samples were collected from greenhouse plants at 30 dpi, immediately ground in liquid nitrogen, and stored in 100 mg aliquots at −80°C.

Time-course sampling for BYV titre quantification: Sugar beet cultivars were first evaluated in a preliminary resistance screening to identify contrasting phenotypes. Based on these results, two cultivars were selected for detailed analysis of virus accumulation kinetics: Masaryk (susceptible) and GZs1 (relevant resistant). Seedlings of both cultivars were grown under controlled environmental conditions (22 - 24°C day/16°C night, 16 h photoperiod, 70% relative humidity). Plants were inoculated with BYV using viruliferous aphids. To characterise virus accumulation kinetics and compare cultivar susceptibility, leaf tissue was collected at 10^{th}, 20^{th}, 30^{th}, 40^{th}, 50^{th}, and 60^{th} dpi. These intervals were selected to capture the early exponential phase and the subsequent plateau or decline typical of BYV titre dynamics. Non-inoculated control plants of both cultivars were sampled at identical time points. All leaf samples were immediately frozen in liquid nitrogen and stored at −80°C until RNA extraction and RT-qPCR analysis.

RNA isolation and cDNA synthesis: Total RNA was isolated from 100 mg of leaf tissue samples that had

been flash-frozen in liquid nitrogen and ground to a fine powder. Extraction was performed using TRIzol™ reagent (*Thermo Scientific*, Waltham, MA, USA) according to the manufacturer's instructions. RNA concentration and purity (A_{260}/A_{280} ratio) were determined using a *NanoDrop™ 2000* spectrophotometer (*Thermo Scientific*). Complementary DNA (cDNA) was synthesized from 1 µg of total RNA using *RevertAid* reverse transcriptase (200 U/µL) and random hexamer primers (*Thermo Scientific*). The reverse transcription reaction was performed using a three-step thermal cycling program: primer annealing at 25°C for 10 min, cDNA synthesis at 42°C for 60 min, and enzyme inactivation at 70°C for 10 min. Following reaction completion, samples were immediately placed on ice.

BYV detection in sugar beet genotypes: Detection of BYV was performed by one-step RT-PCR using the one-enzyme RTX-PCR as described by Hoffmeisterová et al. (2022). The reactions were performed in 25-µl volumes with corresponding negative (water and RNA from healthy plants) and positive controls (RNA from confirmed infected plants). The primer pairs used for BYV detection are listed in Table 1.

Virus titre quantification by RT-qPCR: RT-qPCR was performed using a *LightCycler® 480 Instrument II system* (*Roche*, Basel, Switzerland) to quantify viral titres according to the procedure described in Dráb et al. (2014). Reactions were set up in 384-well plates with a total volume of 12 µL per well, containing 6 µL of 2× *SYBR Green I Master Mix* (*Roche*, Basel, Switzerland), 0.42 µM of each virus-specific primer (Table 1), 4.5 µL of nuclease-free water, and 1 µL of 10-fold diluted cDNA template. The amplification protocol consisted of an initial denaturation at 95°C for 10 min, followed by 40 cycles of denaturation at 95°C for 5 s, primer annealing at 60°C for 30 s, and extension at 72°C for 20 s. Melting-curve analysis was performed between 60°C and 97°C to verify amplification specificity and ensure single amplicon production. Fluorescence was measured at the end of each extension phase, with a final cooling step at 40°C for 10 s.

Standard curves for BYV quantification were constructed using cloned viral sequences. A specific BYV nucleotide sequence (purified PCR amplicon) was ligated into the *pGEM-T Easy* vector (*Promega*, Madison, WI, USA) and introduced into *Escherichia coli* DH5α competent cells. Positive clones were cultured, and plasmid DNA was extracted using the *Plasmid Plus Midi Kit* (*Qiagen*, Hilden, Germany). Plasmid DNA concentrations were quantified spectrophotometrically using a *NanoDrop™ 2000* instrument (*Thermo Scientific*). Serial dilutions (eight-point standard curves) were prepared in 10-fold increments to establish a broad dynamic quantification range. Viral copy numbers were calculated using the formula:

$$\text{pmol of dsDNA} = \frac{(\mu\text{g of dsDNA}) \times 10^6\,\text{pg}/\mu\text{g}}{660\ \text{pg/pmol} \times N_b}$$

where N_b is the number of bases. Avogadro's constant (6.022×10^{23} molecules/mol) was used to estimate the absolute number of molecules (Lee et al., 2006). All standards and biological samples were analysed in triplicate to ensure statistical reliability. Primer efficiency (E) was assessed using serial dilutions and calculated from the slope of the calibration curve according to the equation $E = (10^{-1/\text{slope}} - 1)$ and expressed as a percentage (Pfaffl, 2001). Melting-curve analyses were performed for all primer pairs to confirm the specificity of amplification. Cycle threshold (Ct) values were determined using the *Fit Points* method in *LightCycler® 480* software. Linear regression analysis was performed in *GraphPad Prism 10* (*GraphPad Software*, San Diego, CA, USA) to generate standard curves and calculate viral titres. Samples with Ct values exceeding 35 cycles were classified as below the detection limit. All samples in this study were processed with identical cDNA synthesis and RT-qPCR protocols. Consequently, any systematic RT inefficiency would uniformly affect all measurements across replicates. Therefore, relative quantification of viral genome titres between experimental groups remains valid and reliable. The reported genome copy numbers accurately represent comparative viral accumulation between plant genotypes and treatments. The quantified transcript copy numbers represent viral genome copy equivalents. The estimated BYV copy-equivalent values are expressed as copies per µL of plant cDNA derived from infected leaf samples.

Statistical analysis: The estimated BYV copy-equivalent values (copies per µL plant cDNA) for each genotype were analysed using *GraphPad Prism 10* (*GraphPad Software*). For Phase 1 (30 dpi), differences among genotypes were analysed by one-way *ANOVA* followed by *Tukey*'s multiple-comparison test, using n = 3 - 8 independent plants per genotype (Table 1 Suppl.). For Phase 2, time-course differences between two selected genotypes were analysed using unpaired two-tailed *t*-tests, with n = 3 - 8 independent plants per genotype per time point

Table 1. Primers used in this study.

Primer name	Sequence (5' → 3')	PCR fragment length (bp)	Detection methods	qPCR efficiency	References
BYV_F1	TTTCTAACTGCGACCAGCGT	482 bp	RTX-PCR/Detection		In this study
BYV_R1	CAATTCCTTCCCACCACCGA				
BYV_qF4	CAAAGCTTCGTTCGGTGGTG	181 bp	qPCR	2.03	In this study
BYV_qR4	AGCAATCGGAGGCAGTCTTC				

(Table 2 Suppl.). Results are presented as mean ± standard error. Differences were considered statistically significant at $P < 0.05$.

Results and discussion

We first confirmed BYV infection across all inoculated sugar beet genotypes using a one-enzyme RTX-PCR assay. Absolute RT-qPCR was then used to quantify viral accumulation and compare genotype-dependent differences in viral titres, evaluate the relationship between symptoms and virus load, and resolve contrasting infection kinetics in representative genotypes.

One-enzyme RTX-PCR detected BYV in all inoculated plants (10/10 genotypes, 100% detection rate), with the expected 482 bp amplicons present in positive samples and absent in controls (Fig. 1). Results were fully concordant with conventional RT-PCR, supporting RTX-PCR as a rapid pre-screening method before RT-qPCR quantification, consistent with recent validation studies (Ellefson et al., 2016; Hoffmeisterová et al., 2022; Huang et al., 2025).

Absolute RT-qPCR using BYV_qF4/BYV_qR4 primers showed a linear standard curve across 10^2 - 10^8 dilutions (slope −3.25, R^2 = 0.9976) with 103% amplification efficiency (Fig. 2), enabling robust absolute titre estimation (2.0 being a theoretical perfect efficiency, indicating the doubling of the product with every cycle). The laboratory isolate of BYV was used for the qPCR optimisation, and the primers in the RT-qPCR assay successfully amplified their respective targets (*see* Table 1). This high-quality quantification platform ensured precise viral titre determination (Svec et al., 2015; Bertinelli et al., 2024).

In the greenhouse experiment, BYV copy number was quantified by RT-qPCR in ten sugar beet genotypes at 30 days post-inoculation (dpi) (Fig. 3). Visual symptom assessment showed a genotype-dependent severity gradient that generally matched the RT-qPCR-based virus accumulation pattern. The relatively resistant line GZs2 exhibited the mildest symptoms (mostly green leaves

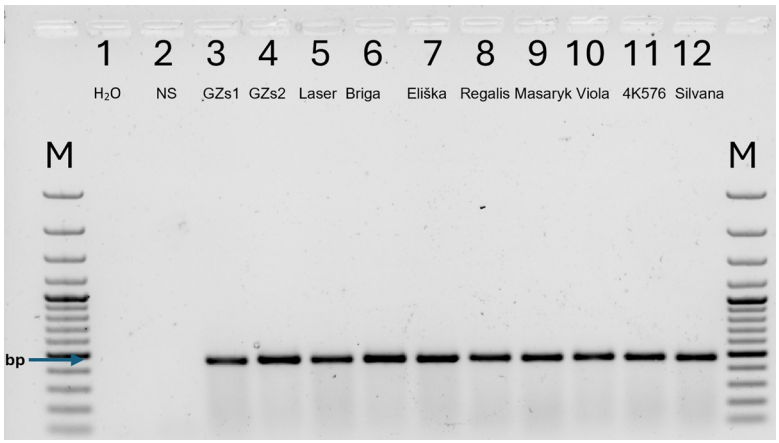

Fig. 1. BYV detection by one-enzyme RTX-PCR using the primer pair BYV_F1/BYV_R1 (482 bp). Lane M: molecular *GeneRuler 100 bp Plus* (*Thermo Fisher Scientific*, Wilmington, DE, USA). Lanes 1: H_2O control, lane 2: negative sample, lanes 3 - 12: BYV positive samples from different sugar beet genotypes.

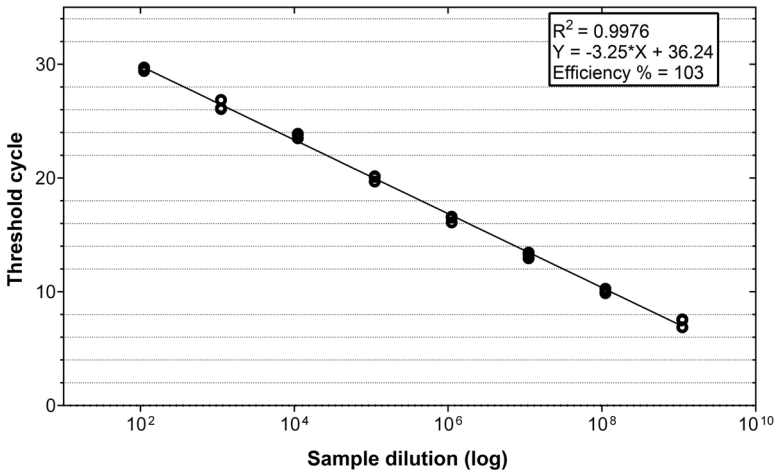

Fig. 2. Standard curve for *SYBR Green I*-based RT-qPCR using BYV_qF4/BYV_qR4 primers on ten-fold serial dilutions of BYV plasmid DNA (10^2 to 10^8 dilutions, triplicate). Linear regression showed a slope of −3.25, R^2 = 0.9976, and 103% efficiency.

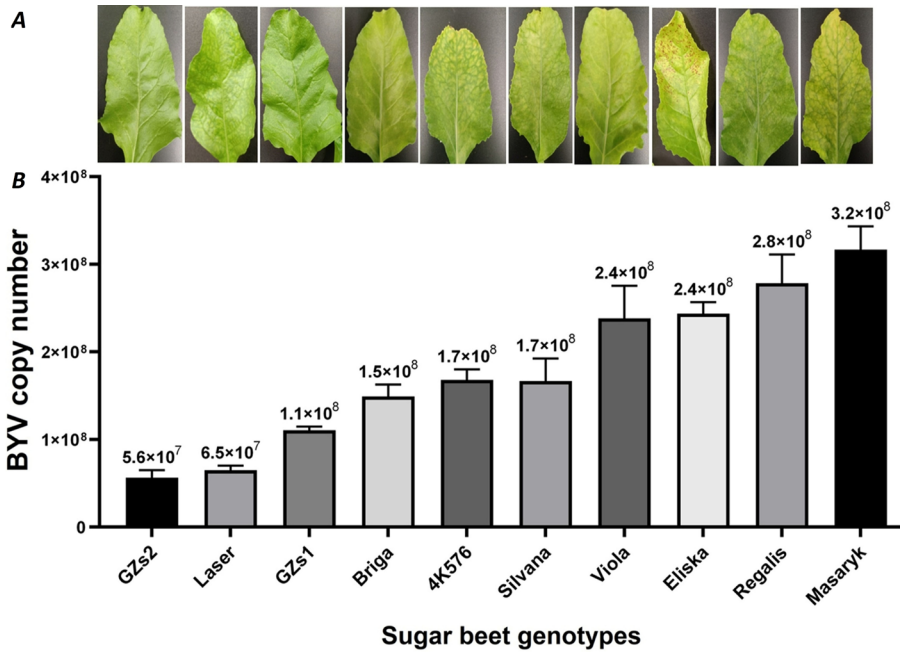

Fig. 3. BYV symptom expression and viral accumulation in sugar beet genotypes at 30 dpi. (*A*) Representative leaves showing the symptoms of BYV infection among the sugar beet genotypes. (*B*) BYV copy number quantified by RT-qPCR at 30 dpi in ten sugar beet genotypes. Bars indicate mean viral titres, and error bars represent standard error (n = 3 - 8 biological replicates). The values above the bars indicate the mean BYV copy number per genotype.

with minimal chlorosis), while the susceptible cultivar Masaryk showed the strongest chlorosis, yellowing, and mottling. High-titre genotypes (Masaryk, Regalis, Eliska, and Viola) displayed more conspicuous symptoms than relatively resistant lines (GZs2, GZs1, and Laser), whereas Briga, 4K576, and Silvana showed intermediate symptom intensity.

Virus accumulation ranged from 5.6×10^7 (GZs2) to 3.2×10^8 copies (Masaryk), and one-way *ANOVA* with *Tukey*'s test identified multiple significant differences among genotypes (Table 1 Suppl.). Studies in other pathosystems have reported weak titre-symptom correlations with R^2 ~0.40, confirming this pattern (Ranabhat et al., 2022). Low-accumulating genotypes likely employ viral restriction mechanisms that suppress early viral replication through antiviral proteins and RNA silencing pathways (Baulcombe, 2004; Ding, 2023). In contrast, high-accumulating genotypes with mild symptoms may possess metabolic tolerance mechanisms that permit viral accumulation while maintaining host function through compensatory pathways (Pagán and García-Arenal, 2018; Paudel and Sanfaçon, 2018). Such responses, combining restriction and tolerance, have been documented in plant–virus interactions (Zvereva and Pooggin, 2012; Cheng and Wang, 2017). This stratification enables rapid germplasm selection for resistance breeding (Nithya et al., 2023; Nandudu et al., 2024). However, temporal kinetic analysis is required to distinguish resistance from tolerance responses and validate the proposed two-level defence framework.

Temporal RT-qPCR profiling revealed fundamentally different host–pathogen dynamics between susceptible (Masaryk) and relatively resistant (GZs1) cultivars. Absolute quantification distinguishes these genotypes based on fundamentally different host–pathogen dynamics (Withycombe et al., 2024). BYV accumulation was monitored across six post-inoculation time points (Fig. 4). Masaryk exhibited rapid viral replication, with copy numbers increasing from 3.1×10^6 at 10 dpi to a peak of 3.7×10^7 at 40 dpi, then declining to 2.5×10^5 by 60 dpi. This pattern indicates severely compromised viral restriction and high susceptibility (Garcia-Ruiz, 2018; Pérez-Cañamás et al., 2022). In contrast, GZs1 showed substantially delayed and suppressed accumulation, rising gradually from 5×10^5 at 10 dpi to 1.8×10^7 at 40 dpi, with sustained levels of 2.3×10^7 at 50 dpi and 1.7×10^7 at 60 dpi. This pattern suggests early active host defence through R gene-mediated siRNA-directed viral silencing (Kang et al., 2005; Soosaar et al., 2005; Ma et al., 2024). Significant differences between cultivars were detected at 10, 20, 30, 40, and 60 dpi (*t*-test, $*P < 0.05$; $** P < 0.01$; $*** P < 0.001$), with Masaryk consistently exhibiting 2- to 6-fold higher viral titres compared to GZs1.

Interestingly, both genotypes converged on similar titres by 50 dpi (~$2.0 - 2.3 \times 10^7$ copies, $P = 0.686$), yet through contrasting pathways: GZs1 through slow, controlled accumulation driven by active host defence; Masaryk through rapid permissive expansion. By 60 dpi, the divergence re-emerged sharply: GZs1 declined to ~1.7×10^7 copies, while Masaryk declined to ~2.5×10^5 copies, a 68-fold difference demonstrating sustained viral control in GZs1. Peak absolute difference occurred at 40 dpi, where Masaryk maintained approximately 2.1-fold higher titres. These contrasting trajectories provide an additional

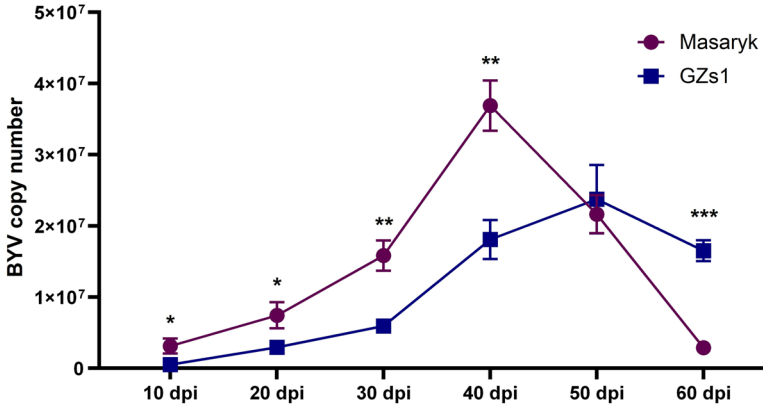

Fig. 4. RT-qPCR was used to determine the BYV copy number in the sugar beet genotypes at specified dpi. Points indicate mean viral titres; error bars show standard error (n = 3 - 8 biological replicates). Statistical significance between genotypes time points was determined by *t*-tests and is indicated by asterisks (* $P < 0.05$, ** $P < 0.01$, *** $P < 0.001$).

quantitative phenotype for ranking genotypes beyond single-time-point titre or visual symptom observations (Kang et al., 2005; Quenouille et al., 2013). Importantly, the timing of viral accumulation is a key determinant of biological impact. Early peak titres, such as those observed in Masaryk at 40 dpi, coincide with critical developmental stages. As a result, these early peaks are more damaging than comparable viral loads reached later in development. In contrast, the delayed accumulation observed in GZs1 occurs when plants are more developmentally resilient. This reduces the physiological and yield consequences of infection. Because aphids acquire BYV while feeding on phloem sap, titre differences have epidemiological significance (Dolja, 2003). Higher viral titres substantially increase aphid acquisition and transmission success (Carroll et al., 2016; Jebakumar et al., 2018). Masaryk's sustained high titres (~3.7 × 10^7 copies at 40 dpi peak) increased phloem accessibility and potentially boosted vector acquisition probability during this critical developmental window. Additionally, early viral dynamics predicted divergent crop impacts (Stevens et al., 2004; Nancarrow et al., 2022). GZs1's early restriction preserved physiological function during critical vegetative and reproductive stages, whereas Masaryk's peak at 40 dpi coincided with maximum developmental vulnerability, amplifying virus-induced carbohydrate deficits and yield loss. RT-qPCR-based kinetic phenotyping proved essential for distinguishing genotype-specific defence mechanisms and predicting both transmission efficiency and crop damage, which visual symptom assessment alone could not reveal.

This study demonstrates the complementary value of a sequential analytical approach: one-enzyme RTX-PCR enables rapid verification of infection across genotypes, single-time-point RT-qPCR provides efficient genotype ranking and screening, and targeted temporal kinetic analysis reveals underlying biological processes and predicts epidemiological and agronomic outcomes. By combining practical scalability with mechanistic understanding, this framework supports informed resistance breeding and enhances understanding of host–pathogen interactions in crop–virus systems.

References

Alquicer, G., Ibrahim, E., Maruthi, M.N. & Kundu, J.K. (2023) Identifying putative resistance genes for barley yellow dwarf virus-PAV in wheat and barley. *Viruses*, 15, 716.

Bass, C., Puinean, A.M., Zimmer, C.T. et al. (2014) The evolution of insecticide resistance in the peach potato aphid, *Myzus persicae*. *Insect Biochemistry and Molecular Biology*, 51, 41-51.

Baulcombe, D. (2004) RNA silencing in plants. *Nature*, 431, 356-363.

Bertinelli, G., Tizzani, L., Luigi, M., Monticelli, S. & Ilardi, V. (2024) Development and validation of one-step reverse transcription-droplet digital PCR for plum pox virus detection and quantification from plant purified RNA and crude extract. *Plants*, 13, 3276.

Borgolte, S., Varrelmann, M. & Hossain, R. (2024) Time point of virus yellows infection is crucial for yield losses in sugar beet, and co-infection with beet mosaic virus is negligible under field conditions. *Plant Pathology*, 73, 2056-2070.

Carroll, J.E., Smith, D.M. & Gray, S.M. (2016) Preferential acquisition and inoculation of PVY^{NTN} over PVY^{O} in potato by the green peach aphid *Myzus persicae* (Sulzer). *Journal of General Virology*, 97, 797-802.

Cheng, X. & Wang, A. (2017) Multifaceted defense and counter-defense in co-evolutionary arms race between plants and viruses. *Communicative & Integrative Biology*, 10, e1341025.

Ding, S.-W. (2023) Transgene silencing, RNA interference, and the antiviral defense mechanism directed by small interfering RNAs. *Phytopathology*, 113, 616-625.

Dolja, V.V. (2003) Beet yellows virus: the importance of being different. *Molecular Plant Pathology*, 4, 91-98.

Dráb, T., Svobodová, E., Ripl, J. et al. (2014) SYBR Green I based RT-qPCR assays for the detection of RNA viruses of cereals and grasses. *Crop and Pasture Science*, 65, 1323-1328.

Ellefson, J.W., Gollihar, J., Shroff, R., Shivram, H., Iyer, V.R. & Ellington, A.D. (2016) Synthetic evolutionary origin of a proofreading reverse transcriptase. *Science*, 352, 1590-1593.

Garcia-Ruiz, H. (2018) Susceptibility genes to plant viruses. *Viruses*, 10, 484.

Hoffmeisterová, H., Kratochvílová, K., Čeřovská, N. et al. (2022) One-enzyme RTX-PCR for the detection of RNA viruses from multiple virus genera and crop plants. *Viruses*, 14, 298.

Hossain, R., Menzel, W., Lachmann, C. & Varrelmann, M. (2021) New insights into virus yellows distribution in Europe

and effects of beet yellows virus, beet mild yellowing virus, and beet chlorosis virus on sugar beet yield following field inoculation. *Plant Pathology*, 70, 584-593.
Hossain, R., Willems, G., Wynant, N., Borgolte, S., Govaerts, K. & Varrelmann, M. (2024) Aphid-mediated beet yellows virus transmission initiates proviral gene deregulation in sugar beet at early stages of infection. *PLoS ONE*, 19, e0311368.
Huang, J., Chen, Y., Zhu, X. et al. (2025) Viral detection in *Phalaenopsis* orchids using high-throughput sequencing and one-step multiplex RT-PCR. *Plant Disease*, 109, 2257-2261.
Ibrahim, E., Rychlá, A., Alquicer, G. et al. (2023) Evaluation of resistance of oilseed rape genotypes to turnip yellows virus. *Plants*, 12, 2501.
Jebakumar, R.M., Balasubramanian, V. & Selvarajan, R. (2018) Virus titre determines the efficiency of *Pentalonia nigronervosa* (Aphididae: Hemiptera) to transmit banana bunchy top virus. *VirusDisease*, 29, 499-505.
Jiménez, J., Tjallingii, W.F., Moreno, A. & Fereres, A. (2018) Newly distinguished cell punctures associated with transmission of the semipersistent phloem-limited beet yellows virus. *Journal of Virology*, 92, e01076-18.
Kanapiya, A., Amanbayeva, U., Tulegenova, Z. et al. (2024) Recent advances and challenges in plant viral diagnostics. *Frontiers in Plant Science*, 15, 1451790.
Kang, B.-C., Yeam, I. & Jahn, M.M. (2005) Genetics of plant virus resistance. *Annual Review of Phytopathology*, 43, 581-621.
Kumar, R., Kaundal, P., Tiwari, R.K. et al. (2022) Establishment of a one-step reverse transcription recombinase polymerase amplification assay for the detection of potato virus S. *Journal of Virological Methods*, 307, 114568.
Kumar, R., Kumar Lal, M., Prasad, P. & Tiwari, R.K. (2023) Editorial: Current advancements in real-time plant pathogen diagnostics: from lab assays to in-field detection. *Frontiers in Plant Science*, 14, 1255654.
Lee, C., Kim, J., Shin, G.S. & Hwang, S. (2006) Absolute and relative QPCR quantification of plasmid copy number in *Escherichia coli*. *Journal of Biotechnology*, 123, 273-280.
Lough, G., Kyriazakis, I., Bergmann, S., Lengeling, A. & Doeschl-Wilson, A.B. (2015) Health trajectories reveal the dynamic contributions of host genetic resistance and tolerance to infection outcome. *Proceedings of the Royal Society B: Biological Sciences*, 282, 20152151.
Ma, X., Zhou, Y., Wu, L. & Moffett, P. (2024) Resistance gene *Ty-1* restricts TYLCV infection in tomato by increasing RNA silencing. *Virology Journal*, 21, 256.
Nancarrow, N., Aftab, M., Hollaway, G., Rodoni, B. & Trębicki, P. (2022) Symptomless turnip yellows virus infection causes grain yield loss in lentil and field pea: A three-year field study in south-eastern Australia. *Frontiers in Plant Science*, 13, 1049905.
Nandudu, L., Sheat, S., Winter, S., Ogbonna, A., Kawuki, R. & Jannink, J.-L. (2024) Genetic complexity of cassava brown streak disease: insights from qPCR-based viral titre analysis and genome-wide association studies. *Frontiers in Plant Science*, 15, 1365132.
Nithya, K., Parameswari, B., Kumar, S. et al. (2023) Prospecting true ScYLV resistance in *Saccharum* hybrid parental population in India by symptom phenotyping and viral titre quantification. *3 Biotech*, 13, 125.
Pagán, I. & García-Arenal, F. (2018) Tolerance to plant pathogens: theory and experimental evidence. *International Journal of Molecular Sciences*, 19, 810.
Paudel, D.B. & Sanfaçon, H. (2018) Exploring the diversity of mechanisms associated with plant tolerance to virus infection. *Frontiers in Plant Science*, 9, 1575.
Pérez-Cañamás, M., Taliansky, M. & Hernández, C. (2022) A viral suppressor of RNA silencing may be targeting a plant defence pathway involving fibrillarin. *Plants*, 11, 1903.
Pfaffl, M.W. (2001) A new mathematical model for relative quantification in real-time RT-PCR. *Nucleic Acids Research*, 29, e45.
Quenouille, J., Montarry, J., Palloix, A. & Moury, B. (2013) Farther, slower, stronger: how the plant genetic background protects a major resistance gene from breakdown. *Molecular Plant Pathology*, 14, 109-118.
Ranabhat, N.B., Bruce, M.A., Fellers, J.P. & Rupp, J.L.S. (2022) A reproducible methodology for absolute viral quantification and viability determination in mechanical inoculations of wheat streak mosaic virus. *Tropical Plant Pathology*, 47, 553-561.
Sharaf, A., Nuc, P., Ripl, J. et al. (2023) Transcriptome dynamics in *Triticum aestivum* genotypes associated with resistance against the wheat dwarf virus. *Viruses*, 15, 689.
Smith, H.G. & Hallsworth, P.B. (1990) The effects of yellowing viruses on yield of sugar beet in field trials, 1985 and 1987. *Annals of Applied Biology*, 116, 503-511.
Soosaar, J.L.M., Burch-Smith, T.M. & Dinesh-Kumar, S.P. (2005) Mechanisms of plant resistance to viruses. *Nature Reviews Microbiology*, 3, 789-798.
Stevens, M., Hallsworth, P.B. & Smith, H.G. (2004) The effects of *Beet mild yellowing virus* and *Beet chlorosis virus* on the yield of UK field-grown sugar beet in 1997, 1999, and 2000. *Annals of Applied Biology*, 144, 113-119.
Sun, B., Li, S., Pi, Z., Wu, Z. & Wang, R. (2024) Assessment of genetic diversity and population structure of exotic sugar beet (*Beta vulgaris* L.) varieties using three molecular markers. *Plants*, 13, 2954.
Svec, D., Tichopad, A., Novosadova, V., Pfaffl, M.W. & Kubista, M. (2015) How good is a PCR efficiency estimate: Recommendations for precise and robust qPCR efficiency assessments. *Biomolecular Detection and Quantification*, 3, 9-16.
Vegvari, C., Hadjichrysanthou, C., Cauët, E. et al. (2016) How can viral dynamics models inform endpoint measures in clinical trials of therapies for acute viral infections? *PLoS ONE*, 11, e0158237.
Withycombe, J., Han, J., MacWilliams, J., Dorn, K.M., Nalam, V.J. & Nachappa, P. (2024) Transcriptomic profiling reveals distinct responses to beet curly top virus (BCTV) infection in resistant and susceptible sugar beet genotypes. *BMC Genomics*, 25, 1237.
Zvereva, A.S. & Pooggin, M.M. (2012) Silencing and innate immunity in plant defense against viral and non-viral pathogens. *Viruses*, 4, 2578-2597.